

A COMPARISON OF MODEL DATA AND OBSERVATIONS IN THE ATMOSPHERIC BOUNDARY LAYER

Eve Wicksteed

January 2020

1 Introduction

It's important for models to be able to simulate the atmosphere fairly accurately for them to be useful to us. The boundary layer (BL) is one of the many things a model should be able to simulate. In order to simulate the boundary layer, models are required to have planetary boundary layer (PBL) schemes in which they parameterize boundary layer processes. These parameterizations need to be made because models are not able to resolve fluxes at the required spatial scales for the BL. This is because the length-scales of eddies are smaller than the model grid spacing (which is normally somewhere between 1 and 4 km). Accuracy in PBL schemes is important because uncertainty and inaccuracies in these forecasts can have impacts on larger scale phenomena (Coniglio et al, 2013).

In order to determine the ability of a model to simulate the BL, I will compare the results of model simulations to observations taken in the boundary layer by atmospheric soundings (sondes). In particular I compare potential temperature predictions under different atmospheric stability conditions for different times of day.

2 Study Area

My area of study is Cape Town, South Africa ($33^{\circ} 55' 31''$ S, $18^{\circ} 25' 26''$ E). I have chosen this location because I am familiar with the area and the weather and thus I am able to have an intuition of the physical processes represented by the data. Cape Town's time zone is GMT+2. This means that the

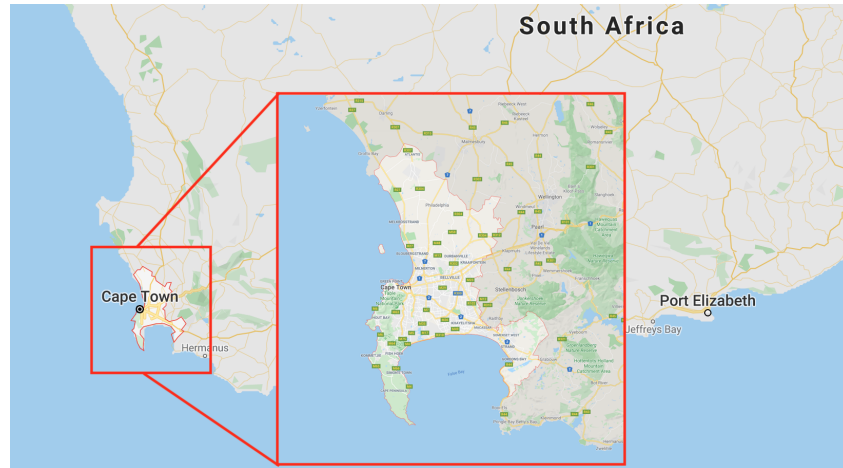


Figure 1: Map of Cape Town, South Africa (Google Maps, 2019)

data at 00z and 12z correspond to 02:00 and 14:00 local time, respectively, and provides examples of soundings both during the day and at night. Although I have specifically chose Cape Town for this project, the methodology could easily be applied to other locations given available data.

3 Data

For this study I use the potential temperature variable to compare the results of model output to observations.

3.1 Model

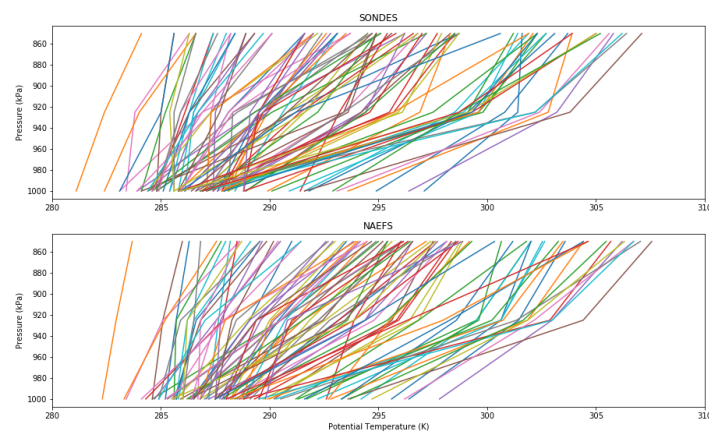


Figure 2: Potential temperature at 1000 kPa, 925 kPa and 850 kPa for soundings and NAEFS

I use two different data sets for this project: model data and observational data (see Figure 2). The

model data is from the North American Ensemble Forecast System (NAEFS; Government of Canada, 2019; archived NAEFS data is available on our team servers). NAEFS is a 42-member ensemble, made up of 21 Canadian members and 21 American members. Each group of 21 members comprises one control member and 20 perturbed members. The control members are the national weather models for Canada: the Global Environmental Multiscale Model (GEM), and for the United States: the Global Forecast System Model (GFS). Perturbations in the model are in initial conditions and the physics schemes (ECC Canada, 2019).

For this project I use only one ensemble member: the GFS control member. The model is initialised at 00z every day and I use daily forecast runs initialised at this time. The forecasts are available for 6-hourly time intervals: 00z, 06z, 12z and 18z. In order to compare model data with corresponding observations, I use only the data available at only 00z and 12z.

The NAEFS models have forecasts for various pressure levels, three of which may be able to capture the boundary layer, depending on boundary layer height: 1000 kPa, 925 kPa and 850 kPa. Thus, these are the levels used in my analysis.

3.2 Observations

Observations are from sounding data, available from the University of Wyoming website (University of Wyoming, 2019). Sounding data is generally available at 00z and 12z and sometimes for Cape Town it is available at 09z. Soundings record data at many points within the PBL. The heights and associated pressure levels at which they are recorded are not consistent. In order to compare soundings with model data, I interpolate the soundings to the 1000 kPa, 925 kPa and 850 kPa pressure levels.

3.3 NAEFS planetary boundary layer scheme

As discussed earlier, the PBL scheme of any model will determine its ability to forecast variables in the boundary layer. What follows will be a brief discussion of the PBL scheme used in the Global Forecast System model.

GFS uses a hybrid Eddy Diffusivity Mass Flux (EDMF) boundary layer parameterization scheme. It is hybrid in the sense that different schemes are used under different conditions in order to improve forecast accuracy. This new hybrid scheme was implemented in 2015 in order to improve the simulation

of PBL growth in the model. The previous scheme that was used is an Eddy Diffusivity Counter Gradient (EDCG) scheme, which tended to under estimate PBL growth, hence the implementation of the EDMF scheme, which takes into account updraft fluxes. However, the EDMF scheme was shown to overestimate mixing in the tropics where the PBL is seldom strongly unstable. Thus, the EDCG scheme is still used in these areas as it better represents vertical mixing under more stable conditions. The BL scheme is selected depending on the stability of the model, making it a hybrid scheme. Stability is determined using z/L where L is the Monin-Obukhov stability parameter. The PBL is classified as strongly unstable (convective) for $z/L < -0.5$, and as weakly and moderately unstable for $0 > z/L > -0.5$, after Sorbjan (1989) (Han et. al., 2016).

How the two schemes differ:

The two schemes differ in their calculation of the vertical turbulent flux. In the counter gradient (CG) scheme the vertical turbulent flux is determined as follows:

$$\overline{w'\phi'} = -K \left(\frac{\partial \bar{\phi}}{\partial z} - \gamma \right) \quad (1)$$

where overbars denote spatial averages, primes are turbulent fluxes, K is the turbulent eddy diffusivity, and γ is the nonlocal CG mixing term due to large nonlocal convective eddies.

Here γ is determined as:

$$\theta = T \left(\frac{P_0}{P} \right)^{R/c_p} \quad (2)$$

which is the surface turbulent flux of the variable, over the velocity scale (w_s) multiplied by BL height (h).

In the mass flux (MF) scheme the nonlocal gradient mixing term, γ , is replaced with a mass flux term and the vertical turbulent flux is calculated by:

$$\overline{w'\phi'} = -K \frac{\partial \bar{\phi}}{\partial z} + M (\phi_u - \bar{\phi}) \quad (3)$$

where the subscript u refers to the updraft properties and M is the updraft mass flux, calculated as:

$$M = a_u (w_u - \bar{w}) \approx a_u w_u \quad (4)$$

and a_u is a small, fixed updraft fractional area that contains the strongest upward vertical velocities.

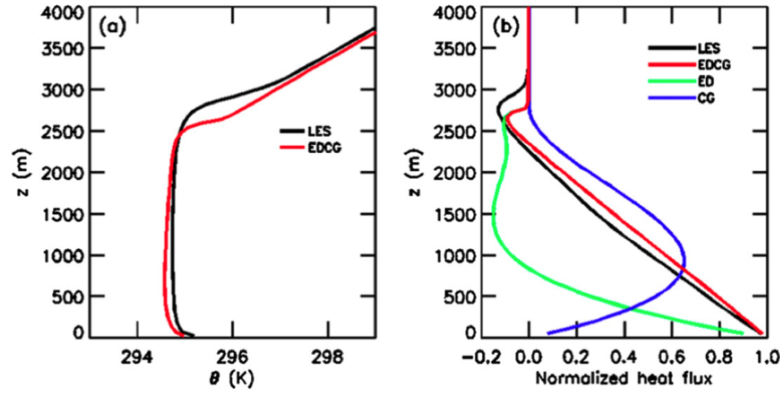


Figure 3: Results of LES model and SCM using the EDCG scheme after an 8-hour simulation. Vertical profiles of (a) potential temperature and (b) total turbulent heat fluxes normalized by surface heat flux are shown, with fluxes broken down into the contributing ED and CG parts (Han et. al., 2016).

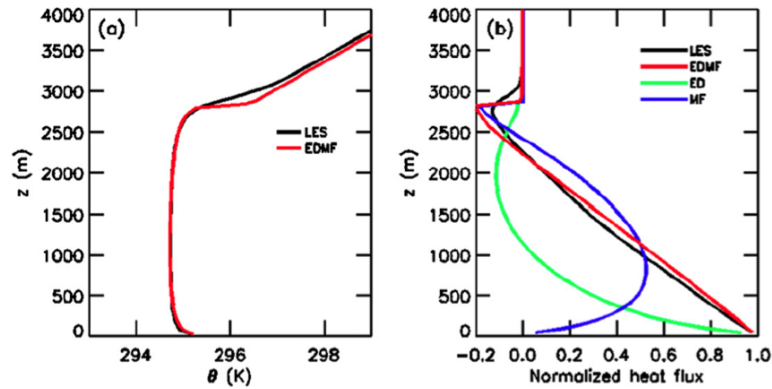


Figure 4: Results of LES model and SCM using the EDCG scheme after an 8-hour simulation. Vertical profiles of (a) potential temperature and (b) total turbulent heat fluxes normalized by surface heat flux are shown, with fluxes broken down into the contributing ED and MF parts. (Han et. al., 2016).

The results of changing this scheme can be seen in Figure 3 and Figure 4. These figures show the comparison of the GFS single column model with a Large Eddy Simulation (LES) from SAM (the

System for Atmospheric Modeling). The vertical profiles of potential temperature and turbulent heat flux are plotted for both models.

Figure 3 shows the EDCG PBL scheme and one can see that the potential temperature does not mix high enough. This is because the SCM under estimates the heat flux in comparison to the LES (b).

Figure 4 shows that the EDMF scheme improves results by better representing updraft fluxes.

4 Methods

The sounding and NAEFS data I downloaded was for multiple times and dates. I made sure that in my comparisons I used only the times that were available in both datasets. This resulted in a dataset of 95 overlapping cases.

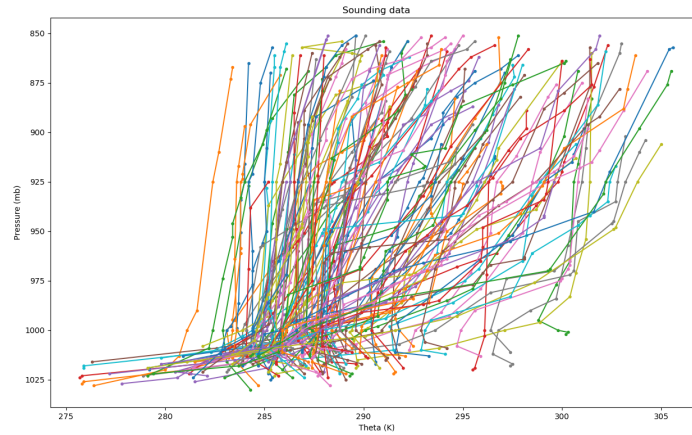


Figure 5: Original sounding data.

I then interpolated potential temperature observations in the soundings to the same pressure levels as the model data (1000 kPa, 925 kPa and 850 kPa). In order to do this I use the SciPy package `scipy.interpolate.interp1d`, which interpolates a 1-D function. Plots of the original sondes and the interpolated sondes can be seen in Figure 5 and Figure 6.

Because potential temperature (θ) is not an output of NAEFS, I calculated θ from the temperature output as follows:

$$\theta = T \left(\frac{P_0}{P} \right)^{R/c_p} \quad (5)$$

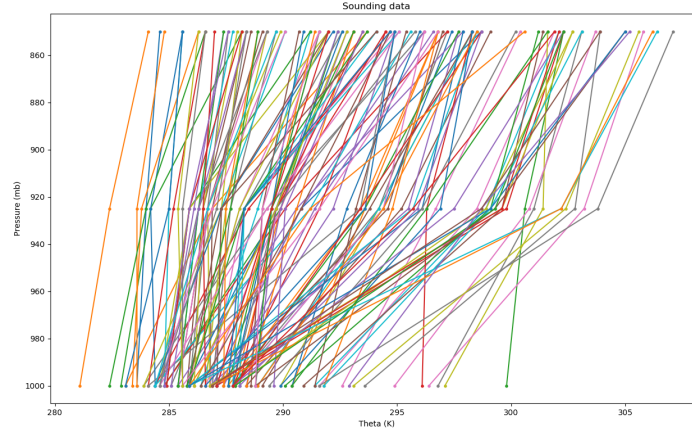


Figure 6: Interpolated sounding data.

where $P0 = 100$ kPa, $R = 287$ J/kg/K and $C_p = 1004$ J/kg/K.

I then classify the atmospheric stability of each case as neutral, stable or unstable. The stability classes are calculated from the potential temperature profiles by looking at the change in θ between the bottom two layers (1000 and 925 kPa). For neutral stability $-0.02 < d < 0.02$, which translates to a change in potential temp of not more than $|0.02|$ Kelvin. For stable conditions $0.02 \leq d$, and for unstable conditions $d \leq -0.02$.

I calculate average potential temperature profiles for different stability conditions and for the different times of day and use this to look at the models ability to simulate the boundary layer.

Finally I calculate some error metrics: mean absolute error (MAE), mean absolute percentage error (MAPE), root mean square error (RMSE), and correlation.

5 Results

In the data there in the observations there are 20 neutral cases and 75 stable cases and in the model data there are 22 neutral cases and 73 stable cases (Figure 7). Unfortunately there were no unstable cases in the data. This is possibly due to the fact that I am using data from Cape Town's winter season (JJA). The winter weather in Cape Town is often stable due to high pressure systems over the south-western part of the country (Preston-Whyte, R.A. and Tyson, 1988).

There are 67 cases at 00z and 28 cases at 12z. The fact that the large majority of cases are at night

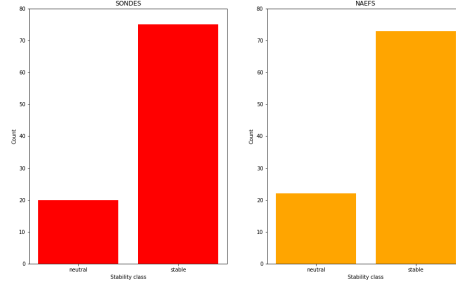


Figure 7: Number of cases by stability class for observations (red) and model data (orange).

also likely contributes to the fact that there are so many stable cases.

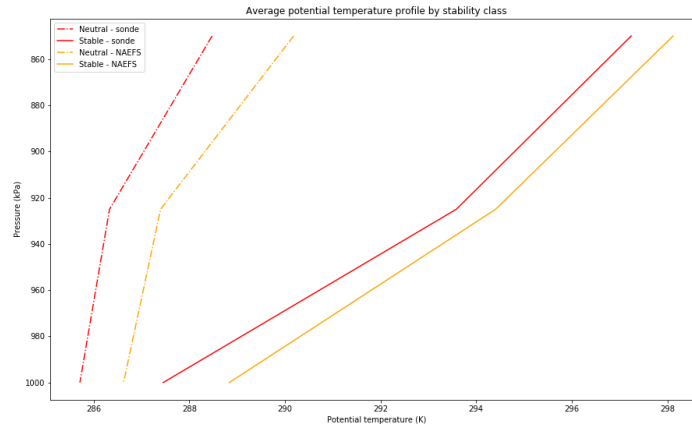


Figure 8: Average potential temperature profiles for observations (red) and model data (orange) for different stability classes.

NAEFS and sounding data for potential temperature show similar patterns, however the average potential temperature ($\bar{\theta}$) in each stability class is lower for the observations than for the model for both neutral and stable atmospheric conditions. It is also seen that in neutral conditions $\bar{\theta}$ is less than in stable cases (Figure 8).

Comparing $\bar{\theta}$ at 00z (02:00 local time) and 12z (14:00 local time) shows that temperatures at night are cooler than during the day, which is to be expected (Figure 9). Night-time data is more similar between model and observations than during the day, where the average potential temperature values follow similar patterns for both datasets but diverge slightly at 1000 kPa and 850 kPa.

Correlations between the datasets are high, with a Pearson correlation coefficient of 0.973 across all the data (Figure 10). Correlations are similar for 850 kPa at 0.975 (highest correlation) and 925 kPa at 0.974 but drop at 1000 kPa to 0.878 (Figure 11). The lower correlation at 1000 kPa seems to be

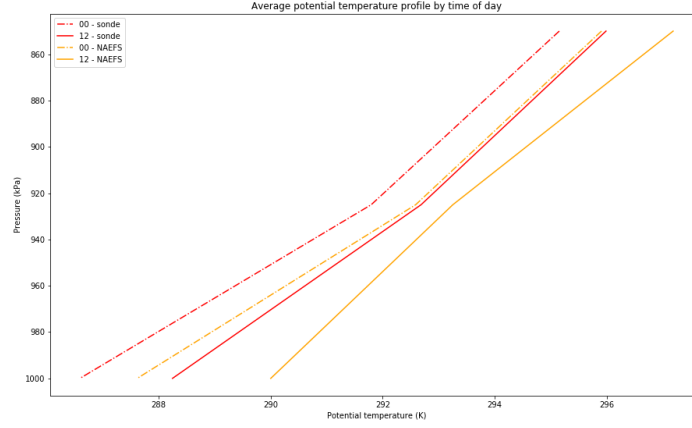


Figure 9: Average potential temperature profiles for observations (red) and model data (orange) for different times of day.

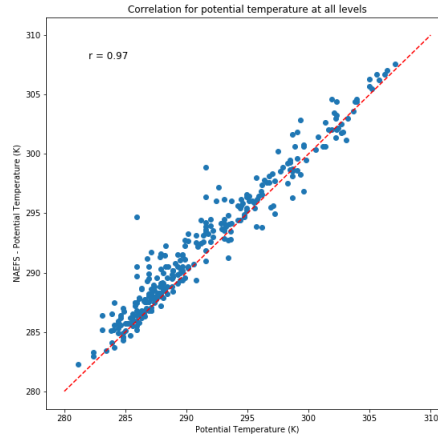


Figure 10: Average correlation between observations and model data for all pressure levels.

caused by the model over-predicting the temperature.

Other error statistics show the same pattern, with the highest error at 1000 kPa. Mean absolute error (MAE) for potential temperature over all levels is 1.22 K and is less than 1.5 K for all levels. Mean absolute percentage error is less than 0.5 % for all levels. Error at 1000 kPa is consistently higher than error at other levels for all error metrics (see 1).

6 Conclusion

The results of this study show that the NAEFS control member (GFS model) simulates the boundary layer (below 850 kPa) fairly well. The model simulations show almost the same number of cases in each

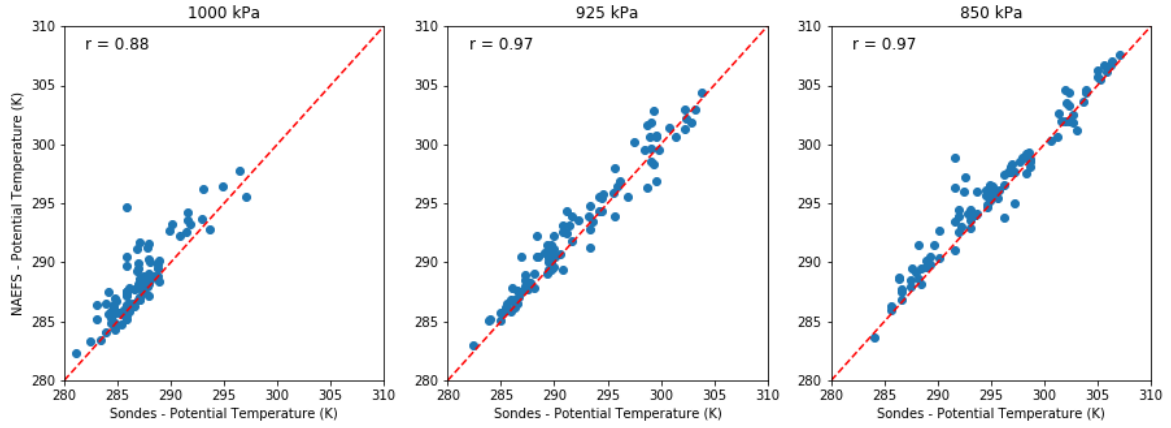


Figure 11: Correlation between observations and model data for individual pressure levels.

Table 1: Table showing error statistics for potential temperature.

	MAE	MAPE	RMSE	Correlation (r)
All levels	1.220	0.419	1.670	0.973
1000 kPa	1.398	0.487	1.941	0.878
925 kPa	1.126	0.385	1.438	0.974
850 kPa	1.136	0.386	1.591	0.975

atmospheric stability class as the observations. In addition, the error metrics show a high correlation between potential temperature in the model and in the observations as well as low RMSE, MAPE and MAE values, indicating a good representation of the real atmosphere by the model. However, model accuracy is lowest at 1000 kPa, which likely means the model is less reliable to forecast data near the surface. This is an area in which the model could improve in order to improve overall accuracy and skill.

One limitation to this study is that I did not compare the hits and misses of the model's stability class predictions. Despite the model predicting a similar number of cases in each stability class to those in the observations, if the model were predicting the classes occurring at the wrong time, this would decrease model accuracy. A further limitation is that I do not have any unstable cases in my dataset. Using more data for a longer period of time, and encompassing other seasons, would improve the results of this study, by providing understanding about the seasonal accuracy of the model simulations. A larger dataset would also provide more robust results and improve the strength of the conclusions.

References

- [1] Coniglio, Michael C and Correia, James and Marsh, Patrick T. *Verification of Convection-Allowing WRF Model Forecasts of the Planetary Boundary Layer Using Sounding Observations*. Weather and Forecasting, 2013.
- [2] Government of Canada *NAEFS - Ensemble Forecast - Environment Canada*. https://weather.gc.ca/ensemble/naefs/index_e.html, 2019.
- [3] Han, Jongil and Witek, Marcin L. and Teixeira, Joao and Sun, Ruiyu and Pan, Hua-Lu and Fletcher, Jennifer K. and Bretherton, Christopher S. *Implementation in the NCEP GFS of a Hybrid Eddy-Diffusivity Mass-Flux (EDMF) Boundary Layer Parameterization with Dissipative Heating and Modified Stable Boundary Layer Mixing*. Weather and Forecasting, 2016.
- [4] University of Wyoming. *Upper air sounding*. <http://weather.uwyo.edu/upperair/sounding.html>, 2019.